EBOLA

mAbs and Ad-Vectored IFN-α Therapy Rescue Ebola-Infected Nonhuman Primates When Administered After the Detection of Viremia and Symptoms

Xiangguo Qiu,[1] Gary Wong,[1,2] Lisa Fernando,[1] Jonathan Audet,[1,2] Alexander Bello,[1,2] Jim Strong,[1] Judie B. Alimonti,[1,2] Gary P. Kobinger[1,2,3,4]*

ZMAb is a promising treatment against Ebola virus (EBOV) disease that has been shown to protect 50% (two of four) of nonhuman primates (NHPs) when administered 2 days post-infection (dpi). To extend the treatment window and improve protection, we combined ZMAb with adenovirus-vectored interferon-α (Ad-IFN) and evaluated efficacy in EBOV-infected NHPs. Seventy-five percent (three of four) and 100% (four of four) of cynomolgus and rhesus macaques survived, respectively, when treatment was initiated after detection of viremia at 3 dpi. Fifty percent (two of four) of the cynomolgus macaques survived when Ad-IFN was given at 1 dpi, followed by ZMAb starting at 4 dpi, after positive diagnosis. The treatment was able to suppress viremia reaching ~10^5 $TCID_{50}$ (median tissue culture infectious dose) per milliliter, leading to survival and robust specific immune responses. This study describes conditions capable of saving 100% of EBOV-infected NHPs when initiated after the presence of detectable viremia along with symptoms.

INTRODUCTION

Ebola virus is an aggressive human pathogen, which is responsible for sporadic but deadly outbreaks of hemorrhagic fever, with *Zaire ebolavirus* (EBOV) being the most lethal and causing up to 90% mortality in untreated humans (*1*). Treatment for infected patients is supportive in nature with simple hydration, administration of vitamins, and control of possible co-infections. There is no licensed vaccine or treatment. Over the last year, several studies have demonstrated potential for effective antibody-based therapy of EBOV infection. The successful treatment of nonhuman primates (NHPs) after challenge with concentrated, polyclonal immunoglobulin G (IgG) from NHP survivors of EBOV infection demonstrated that antibody treatments can be protective after exposure to the virus (*2*). In a separate study, rhesus macaques were treated starting 1 day before challenge with three intravenous doses at 50-mg monoclonal antibody (mAb) mixture per animal, consisting of two human-mouse chimeric mAbs, ch133 and ch226, with strong EBOV-neutralizing activity. One of three animals survived challenge with no clinical symptoms and reduced viremia, but significant decreases in circulating mAb levels were observed in the two nonsurvivors with a concomitant increase in viral load (*3*). Another group produced large amounts of three anti-EBOV human-mouse chimeric mAbs (c13C6, h-13F6, and c6D8) in *Nicotiana benthamiana*. Two of three infected rhesus macaques were protected when given a mixture of the three mAbs (MB-003) totaling 50 mg/kg per dose beginning at 1 or 2 days post-infection (dpi), with three additional identical doses spaced 2 to 3 days apart. Surviving animals experienced little to no viremia and had few clinical symptoms (*4*). Another promising mAb combination therapy consisting of 1H3, 2G4, and 4G7 murine monoclonals (ZMAb) demonstrated complete survival in four cynomolgus macaques when three doses at 25 mg/kg were administered beginning at 1 dpi. The same treatment initiated at 2 dpi resulted in two of four survivors, with protected NHPs demonstrating EBOV-specific humoral and cell-mediated immune responses (*5*). The successful protection of macaques with mAbs highlights the critical role of antibodies in the control of EBOV replication in vivo and supports their use as a clinical modality to treat EBOV infection in humans.

This study aims to build on the previous work by extending the post-exposure treatment window beyond current limits in NHPs. ZMAb was combined with Ad-IFN (*6*), a replication-defective recombinant human adenovirus serotype 5 (AdHu5) expressing consensus human interferon-α (IFN-α). Ad-IFN has been developed as a broad-spectrum antiviral and shown to enhance the EBOV-specific adaptive immune response as well as inhibit viral replication (*7*). It also enhances the protective efficacy of ZMAb treatments in guinea pigs, a lower animal model of EBOV infection (*8*). On this basis, we investigated the protective efficacy of the combined ZMAb and Ad-IFN treatment in rhesus and cynomolgus macaques, administered either at the same time or with Ad-IFN first, followed by ZMAb days later. This later experimental design was to mimic an early response to a potential exposure without a diagnosis followed by a final treatment specifically targeting EBOV supported by a positive laboratory-confirmed diagnosis. Survival, clinical signs, and specific immune responses to EBOV were examined after challenge.

RESULTS

Survival and clinical observations

Combination therapy with ZMAb and Ad-IFN was evaluated previously in guinea pigs, where initiation of treatment at 3 dpi provided 100% survival. Early administration of Ad-IFN within 1 dpi permitted later mAb use up to 7 dpi with full survival, constituting a significant

[1]Special Pathogens Program, National Microbiology Laboratory, Public Health Agency of Canada, Winnipeg, Manitoba R3E 3R2, Canada. [2]Department of Medical Microbiology, University of Manitoba, Winnipeg, Manitoba R3E 0J9, Canada. [3]Department of Immunology, University of Manitoba, Winnipeg, Manitoba R3E 0T5, Canada. [4]Department of Pathology and Laboratory Medicine, University of Pennsylvania School of Medicine, Philadelphia, PA 19104, USA.
*Corresponding author. E-mail: Gary.Kobinger@phac-aspc.gc.ca

improvement over either treatment alone (*8*). Three separate studies aimed at enhancing protective efficacy were conducted in NHPs. The first experiment (Cyno72h, groups A and B) consisted of four cynomolgus macaques receiving three doses of ZMAb (50 mg/kg) intravenously at 3-day intervals, beginning at 3 dpi after an uniformly lethal intramuscular challenge with 1000 plaque-forming units (PFU) of EBOV. NHPs were supplemented with Ad-IFN (1×10^9 PFU/kg) intramuscularly at the time of the first dose (Fig. 1A). Control mouse IgG and phosphate-buffered saline (PBS) animals (B1 and B2, respectively) succumbed to disease with symptoms typical of EBOV at 5 dpi. A control animal treated only with Ad-IFN was not performed because a previous study had already shown it to be ineffective in rescuing NHPs from lethal EBOV infection (*9*). Control IgG was not combined with Ad-IFN as a control because the administration of an isotype control did not delay the time to death in a previous study (*8*). Consequently, survival rates would not be expected to differ from animals receiving Ad-IFN alone. Three of four NHPs (A1, A3, and A4) survived challenge with mild signs of disease (Table 1), with A2 experiencing a significant delay in time to forced euthanasia (25 dpi; $P = 0.01$ using the log-rank test for survival and comparing group A to B + D, total $n = 8$) (Fig. 1B). Viremia was detected in all animals beginning at 3 dpi by $TCID_{50}$ (median tissue culture infectious dose) and qRT-PCR (quantitative reverse transcription polymerase chain reaction) from blood sampled just before treatment administration (Fig. 1C and tables S1 and S2). Viremia decreased to undetectable levels by 16 dpi after completion of the treatment regimens but was uncontrollable in both control NHPs. Clinical scores and rectal temperatures remained normal for all surviving animals (Fig. 1, D and E, and tables S3 and S4). Viremia in A2 rebounded to high levels a few days preceding euthanasia, with EBOV also detected in its cerebrospinal fluid at 5.8×10^8 genome equivalent copies (GECs)/ml. Notable changes in hematology and blood chemistry included leukocytopenia, thrombocytopenia, and elevated liver enzymes (ALT/ALP) in nonsurvivors on the date of euthanasia, which indicate liver dysfunction commonly associated with EBOV infection (*9*). Survivors exhibited leukocytopenia and thrombocytopenia but did not exhibit blood chemistry abnormalities (Fig. 1, F to I, and tables S5 to S8).

The second experiment (Cyno96h, groups C and D) focused on extending the EBOV treatment window. Ad-IFN was first administered as a broad-spectrum antiviral when viral load is under the limit of detection of known assays, and then followed by EBOV-specific ZMAb treatment upon detection of viremia and fever. This protocol was designed to mimic a situation where suspected but unconfirmed exposures to EBOV can be managed preventively before specific treatment is administered after a confirmed diagnosis. A group of four cynomolgus macaques were given the same dose of Ad-IFN at 1 dpi and ZMAb regimens beginning at 4 dpi, when both viremia and fever can be detected in the animals (Fig. 2A). Control mouse IgG and PBS animals (D1 and D2, respectively) succumbed to EBOV disease at 5 and 6 dpi. Two of four NHPs (C2 and C3) survived infection, but both developed additional signs of disease before fully recovering by 28 dpi. C1 died at 6 dpi, whereas C4 displayed a significantly extended time to death (23 dpi) (Fig. 2B; $P = 0.0397$ using the log-rank test for survival and comparing group C to B + D, total $n = 8$). No viremia was detected in animal C4 at time of death; its oral, nasal, and rectal swabs were also negative in qRT-PCR for EBOV (table S9). The blood was then sent for amplification and sequencing of 16*S* ribosomal DNA (rDNA) to verify whether it contracted a secondary infection. No 16*S* rDNA could be detected (table S9). The cause of death in animal C4 is unknown. It was notable that C1 exhibited viremia levels of 3.16×10^6 $TCID_{50}$ at 4 dpi, at least 1 log higher than the other treated animals, but ZMAb was effective in reducing viremia in survivors to undetectable levels by 14 dpi. Unexpectedly, viremia was not observed in C4 at time of forced euthanasia (Fig. 2C and tables S1 and S2).

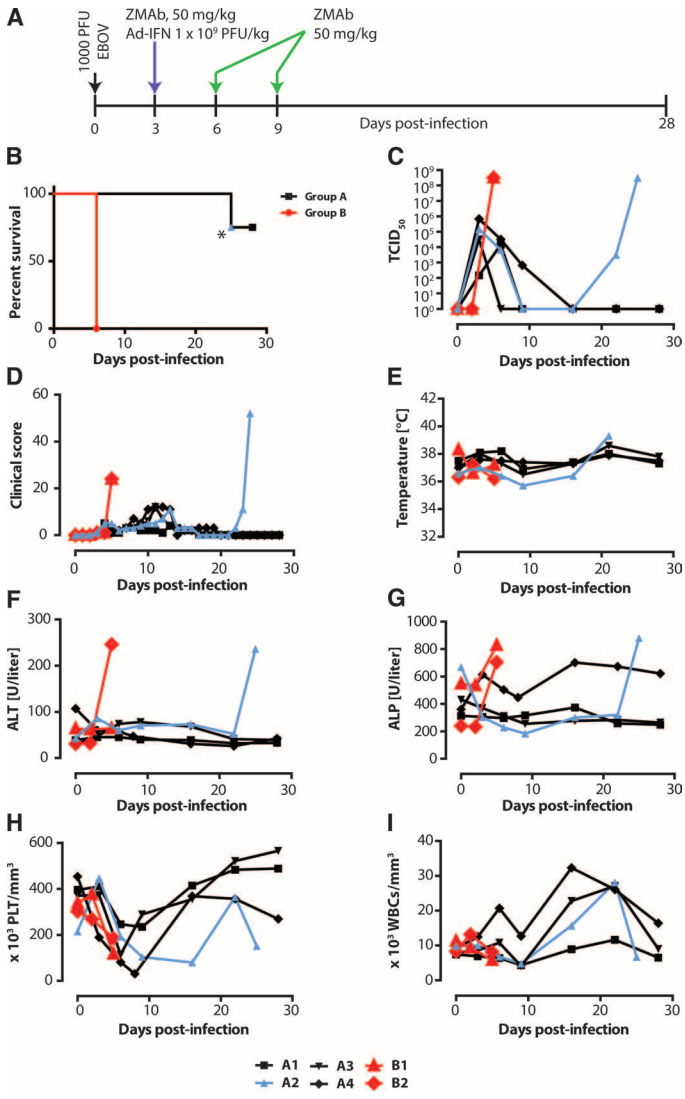

Fig. 1. Survival and clinical overview of cynomolgus macaques treated with mAbs and Ad-IFN starting at 3 dpi. (**A**) Animals (Cyno72h) were challenged with EBOV (red arrow) and administered intravenously with ZMAb and intramuscularly with Ad-IFN (blue arrow) at 3 dpi and then two more intravenous ZMAb treatments at 6 and 9 dpi (green arrows). Control animals received either PBS (B1) or mouse IgG (B2). (**B** to **E**) Animals were sampled on treatment and postmortem days in addition to 14, 21, and 28 dpi and examined for (B) survival [*$P = 0.0253$, log-rank test Cyno72h versus two controls (B1 and B2)], (C) viremia, (D) clinical score, and (E) rectal temperature. (**F** to **I**) Variations in blood biochemistry and hematological levels were recorded for (F) alanine aminotransferase (ALT), (G) alkaline phosphatase (ALP), (H) platelets (PLT), and (I) white blood cells (WBCs). Animals A1 to A4 received the treatment; animals B1 and B2 were the controls.

Table 1. Clinical findings on days 1 to 28 after EBOV challenge. Hypothermia was defined as below 35°C. Fever was defined as >1.0°C higher than baseline. Mild rash was defined as focal areas of petechiae covering <10% of the skin, moderate rash as areas of petechiae covering 10 to 40% of the skin, and severe rash as areas of petechiae and/or ecchymosis covering >40% of the skin. Leukocytopenia and thrombocytopenia were defined as a >30% decrease in numbers of WBCs and platelets, respectively. Leukocytosis and thrombocytosis were defined as a twofold or greater increase in numbers of WBCs and platelets over baseline, where WBC count >11.000. ↑, two- to threefold increase; ↑↑, four- to fivefold increase; ↑↑↑, greater than fivefold increase; ↓, two- to threefold decrease; ↓↓, four- to fivefold decrease; ↓↓↓, greater than fivefold decrease. ALB, albumin; AMY, amylase; TBIL, total bilirubin; BUN, blood urea nitrogen; PHOS, phosphate; CRE, creatinine; GLU, glucose; GLOB, globulin; —, no change.

Animal ID	Treatments	Findings	Status
Cyno72h			
A1	3 dpi Ad-IFN and 50 mg/kg mAb	Leukocytopenia (9 dpi), thrombocytopenia (6, 9 dpi)	Survived
		—	
A2	3 dpi Ad-IFN and 50 mg/kg mAb	Fever (22 dpi), leukocytopenia (6, 9, 25 dpi), leukocytosis (22 dpi), thrombocytopenia (9, 16 dpi), thrombocytosis (3 dpi)	Died at 25 dpi
		ALT↑ (3 dpi), ALP↑↑↑ (25 dpi), AMY↑ (3, 6, 16 dpi), BUN↓ (9 dpi), CRE↓ (25 dpi), GLU↑↑↑ (25 dpi)	
A3	3 dpi Ad-IFN and 50 mg/kg mAb	Fever (22 dpi), leukocytopenia (9 dpi), leukocytosis (16, 22 dpi), thrombocytopenia (6 dpi)	Survived
		ALB↓ (16 dpi), ALT↑ (6, 9, 16 dpi)	
A4	3 dpi Ad-IFN and 50 mg/kg mAb	Leukocytosis (6, 16, 22 dpi), thrombocytopenia (3, 6, 8, 28 dpi)	Survived
		TBIL↑ (6, 8 dpi)	
B1	2 dpi mAb control	Severe rash (5 dpi), leukocytopenia (5 dpi), thrombocytopenia (5 dpi)	Died at 5 dpi
		TBIL↑ (5 dpi), BUN↑ (5 dpi), CRE↑↑ (5 dpi)	
B2	2 dpi PBS control	Severe rash (5 dpi), thrombocytopenia (5 dpi)	Died at 5 dpi
		ALP↑ (5 dpi), ALT↑↑↑ (5 dpi), BUN↑ (5 dpi), CRE↑↑ (5 dpi)	
Cyno96h			
C1	1 dpi Ad-IFN and 4 dpi 50 mg/kg mAb	Fever (4 dpi), severe rash (6 dpi), leukocytopenia (6 dpi), thrombocytopenia (4, 6 dpi)	Died at 6 dpi
		ALT↑↑↑ (6 dpi), AMY↑↑↑ (6 dpi), TBIL↑↑ (6 dpi), BUN↑↑ (6 dpi), PHOS↑↑↑ (6 dpi), CRE↑↑↑ (6 dpi), GLU↑↑↑ (6 dpi)	
C2	1 dpi Ad-IFN and 4 dpi 50 mg/kg mAb	Fever (21 dpi), mild rash (14 dpi), leukocytosis (10, 21, 28 dpi), thrombocytopenia (7, 10, 14 dpi)	Survived
		ALP↑ (14, 21, 28 dpi), GLU↑ (4, 7, 10 dpi)	
C3	1 dpi Ad-IFN and 4 dpi 50 mg/kg mAb	Hypothermia (14 dpi), leukocytopenia (7, 14 dpi), thrombocytopenia (4, 7, 10, 14, 21 dpi)	Survived
		CRE↑ (7 dpi)	
C4	1 dpi Ad-IFN and 4 dpi 50 mg/kg mAb	Hypothermia (10, 23 dpi), leukocytopenia (7, 14 dpi), leukocytosis (21 dpi), thrombocytopenia (7, 10, 14 dpi)	Died at 23 dpi
		BUN↑ (23 dpi), GLU↑ (23 dpi), GLOB↑ (21, 23 dpi)	
D1	1 dpi PBS and 4 dpi mAb control	Severe rash (6 dpi), leukocytopenia (6 dpi), thrombocytopenia (4, 6 dpi)	Died at 6 dpi
		ALP↑ (6 dpi), TBIL↑ (6 dpi), GLU↑ (6 dpi)	
D2	1 dpi PBS and 4 dpi PBS control	Severe rash (6 dpi), leukocytopenia (5 dpi), leukocytosis (2 dpi), thrombocytopenia (4, 5 dpi)	Died at 5 dpi
		ALB↓↓↓ (5 dpi), ALP↑↑↑ (5 dpi), ALT↑↑↑ (5 dpi), AMY↑↑ (5 dpi), BUN↑↑ (5 dpi), PHOS↑↑↑ (5 dpi), CRE↑↑↑ (5 dpi), GLU↓ (5 dpi), GLOB↓↓↓ (5 dpi)	
Rhesus72h			
E1	3 dpi Ad-IFN and 50 mg/kg mAb	—	Survived
E2	3 dpi Ad-IFN and 50 mg/kg mAb	Thrombocytopenia (6 dpi)	Survived
E3	3 dpi Ad-IFN and 50 mg/kg mAb	—	Survived
E4	3 dpi Ad-IFN and 50 mg/kg mAb	Leukocytosis (3, 9 dpi)	Survived
F1	3 dpi mAb control	Moderate rash (6 dpi), leukocytopenia (7 dpi), thrombocytopenia (6, 7 dpi), ALB↑ (7 dpi), ALT↑↑↑ (6, 7 dpi), TBIL↑ (6, 7 dpi), BUN↑ (6, 7 dpi), PHOS↑↑ (7 dpi), CRE↑↑ (6 dpi) ↑↑↑ (7 dpi), GLU↓ (7 dpi), GLOB↑↑↑ (7 dpi)	Died at 7 dpi
F2	3 dpi Ad-IFN only control	Mild rash (6 dpi), moderate rash (9 dpi), leukocytosis (3 dpi), thrombocytopenia (6, 9 dpi)	Died at 9 dpi
		ALT↑↑ (6, 7 dpi), PHOS↓ (9 dpi)	

Clinical scores were most prominent between 6 and 15 dpi, when rectal temperatures fluctuated for both surviving animals with C2 and C3 developing fever and hypothermia, respectively (Fig. 2, D and E, and tables S3 and S4). Notable changes in hematology and blood chemistry include leukocytopenia, thrombocytopenia, and elevated ALT/ALP in nonsurviving animals on the date of euthanasia. Leukocytopenia was detected in survivor C3, whereas both survivors exhibited thrombocytopenia but no abnormal changes in their blood chemistry. Surprisingly, C4 did not exhibit abnormal liver function or platelet count before euthanasia. Leukocytosis was reported at 21 dpi but had dropped to within normal range before the humane endpoint for euthanasia was reached (Fig. 2, F to I, and tables S5 to S8).

In the third experiment (Rhesus72h, groups E and F), a group of four rhesus macaques were administered the same treatment protocol

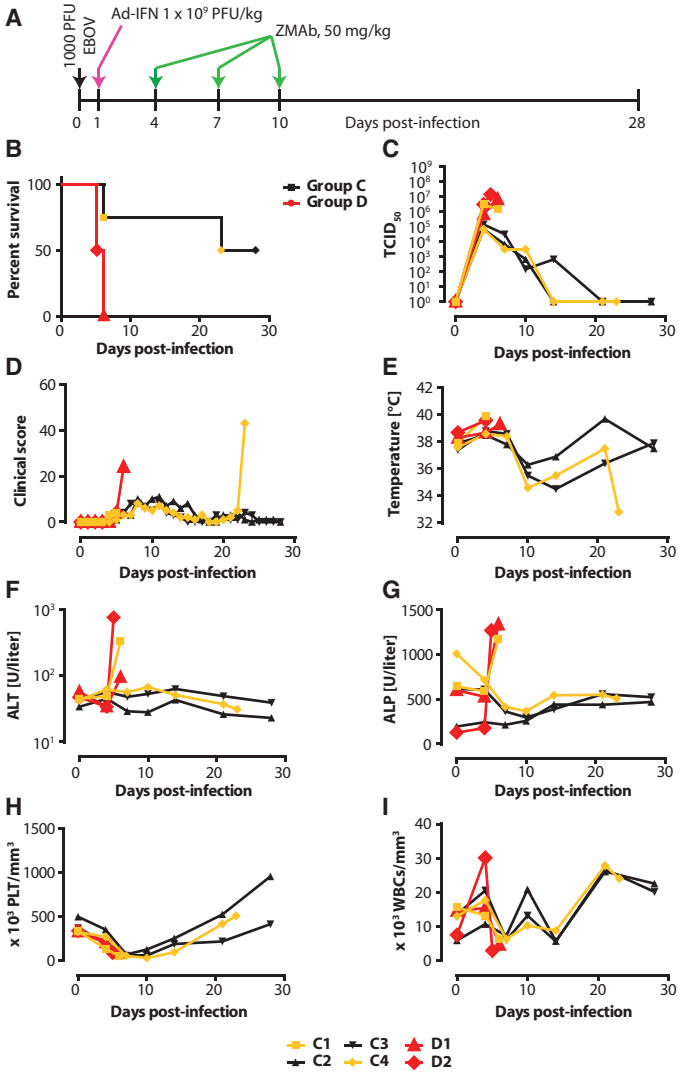

Fig. 2. Survival and clinical overview of cynomolgus macaques treated with Ad-IFN at 1 dpi, and then mAbs starting at 4 dpi. (**A**) Animals (Cyno96h) were challenged with EBOV (red arrow) and administered intramuscularly with Ad-IFN (purple arrow) at 1 dpi and then three intravenous ZMAb treatments at 4, 7, and 10 dpi (green arrows). Control animals received either PBS (D1) or PBS at 1 dpi followed by mouse IgG at 4 dpi (D2). (**B** to **E**) Animals were sampled on treatment and postmortem days in addition to 14, 21, and 28 dpi and examined for (B) survival [$P = 0.0624$, log-rank test for survival comparing Cyno96h to two controls (D1 and D2)], (C) viremia, (D) clinical score, and (E) rectal temperature. (**F** to **I**) Variations in blood biochemistry and hematological levels were recorded for (F) ALT, (G) ALP, (H) platelets, and (I) WBCs. Animals C1 to C4 received the treatment; animals D1 and D2 were the controls.

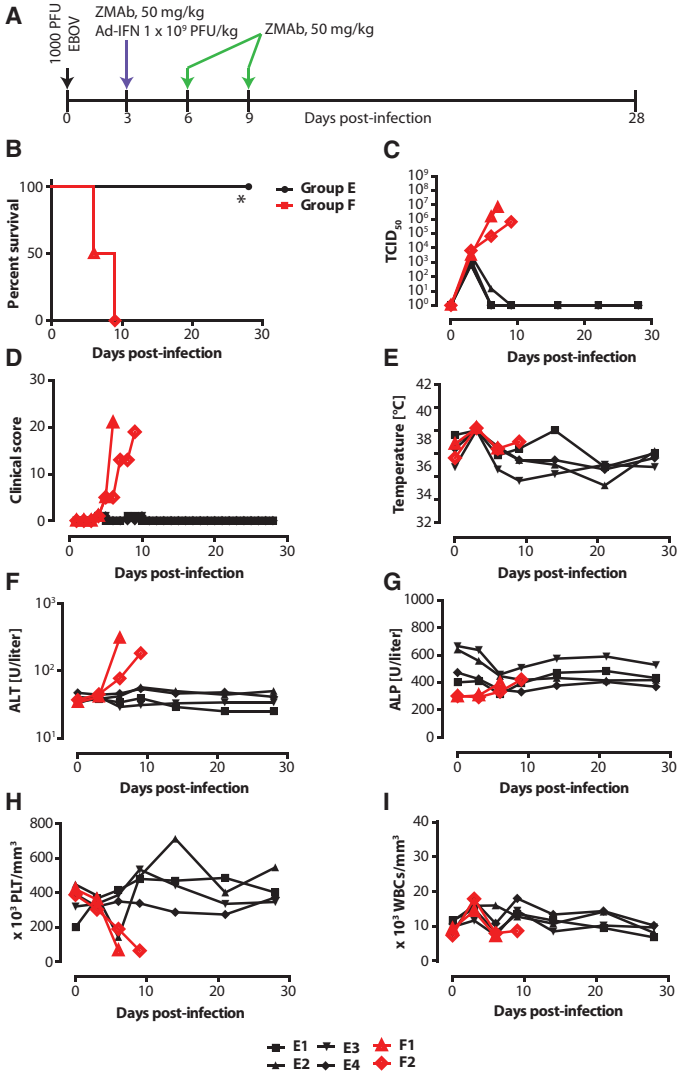

Fig. 3. Survival and clinical overview of rhesus macaques treated with mAbs and Ad-IFN starting at 3 dpi. (**A**) Animals (Rhesus72h) were challenged with EBOV (red arrow) and administered intravenously with ZMAb and intramuscularly with Ad-IFN (blue arrow) at 3 dpi and then two more intravenous ZMAb treatments at 6 and 9 dpi (green arrows). One control animal received mouse IgG (F1), and the other received Ad-IFN alone (F2). (**B** to **E**) Animals were sampled on treatment and postmortem days in addition to 14, 21, and 28 dpi and examined for (B) survival [*$P = 0.0177$, log-rank test for survival comparing Rhesus72h to two controls (F1 and F2)], (C) viremia, (D) clinical score, and (E) rectal temperature. (**F** to **I**) Variations in blood biochemistry and hematological levels were recorded for (F) ALT, (G) ALP, (H) platelets, and (I) WBCs. Animals E1 to E4 received the treatment; animals F1 and F2 were the controls.

as Cyno72h animals. Here, control animals (F1 and F2) were given control mouse IgG or Ad-IFN alone, respectively (Fig. 3A). F1 and F2 succumbed to infection at 7 and 9 dpi, respectively, whereas all treated animals (E1 to E4) survived the challenge with low to no observable clinical signs of disease 1 week after treatment initiation (Fig. 3B; $P = 0.0177$ using the log-rank test and comparing group E to group F, total $n = 6$). Viremia and a fever of 40°C or above were detected at 3 dpi before treatment in all animals. No permanent abnormalities were observed with clinical scores, temperatures, blood chemistry, or hematology among survivors (Fig. 3, C to I, and tables S1 to S8).

EBOV glycoprotein–specific antibody response

Immune responses were monitored after challenge to determine whether the ZMAb and Ad-IFN combination treatment can sufficiently control EBOV replication until the animals are able to generate their own protective immunity. Characterization of humoral responses involved the quantification of total serum EBOV glycoprotein (GP)–specific IgM and IgG by enzyme-linked immunosorbent assay (ELISA) or EBOV-specific neutralizing antibody (nAb) assays. Total NHP EBOV-GP–specific IgM levels were detected within 4 dpi in all survivors and remained constant until 28 dpi (Fig. 4, A to C, and table S10), ranging from ~10^3 to ~10^5 reciprocal dilutions. In contrast, control animals exhibited low to undetectable levels with the exception of the Ad-IFN–treated F2 at its humane endpoint (9 dpi). In nonsurviving animals, IgM levels were comparable to survivors at 3 and 4 dpi in A2 and C4, respectively, but C1 had IgM levels below the detection limit of the assay.

Total NHP EBOV-GP–specific IgG levels were detected from all surviving NHPs by 6 dpi and increased until 28 dpi (Fig. 4, D to F, and table S11). Control animals had undetectable levels of IgG at the time of euthanasia, with the exception of F2 at 9 dpi. Cynomolgus macaques from the Cyno72h group exhibited 2 log higher reciprocal dilutions of IgG than those from Cyno96h by 16 dpi (~10^6 versus ~10^4 reciprocal dilutions), although Cyno96h survivors reached comparable IgG levels by 28 dpi. In the Rhesus72h group, IgG levels were variable among survivors with final levels reaching between ~10^4 and ~10^6 reciprocal dilutions. Among nonsurviving animals, A2 exhibited IgG levels 2.5 log lower than the survivors in this treatment group, and did not appreciably increase in titer throughout the experiment. C1 and C4 both exhibited IgG titer progression comparable to survivors in their treatment group until the time of euthanasia. Serum EBOV-specific nAbs were observed and peaked at 6 to 9 dpi in all ZMAb-treated animals, before diminishing to undetectable levels by 16 dpi. Control animals showed low to undetectable nAb titers after challenge (fig. S1 and table S12).

EBOV-GP–specific T cell response

The EBOV-GP–specific T cell response was examined in survivor peripheral blood mononuclear cells (PBMCs) at 21 dpi with IFN-γ enzyme-linked immunospot (ELISpot) assays and intracellular cytokine staining (ICS) flow cytometry. IFN-γ ELISpots demonstrated that the response to EBOV-GP was comparable in the Cyno72h (Fig. 5A and table S13) and Cyno96h studies (Fig. 5B and table S13), with three of four animals (A1, A3, and A4) and three of three animals (C2, C3, and C4) secreting IFN-γ at an average of 911 and 1018 spot-forming units (SFUs)/10^6 PBMCs, respectively. The highest response was observed in the Rhesus72h group (Fig. 5C and table S13), where four of four animals (E1 to E4) secreted IFN-γ at an average of 2586 SFUs/10^6 PBMCs.

The ICS assay provided a relative comparison between treatment groups of the EBOV-GP–specific $CD4^+$ (Fig. 5D and tables S14 to S18) or $CD8^+$ (Fig. 5E and tables S19 to S23) T cells that were either $CD107a^+$, IFN-γ^+, IL-2^+ (interleukin-2–positive), or IL-4^+. The Cyno72h group had higher percentages of $CD4^+$ cells expressing CD107a, IFN-γ, IL-2, or IL-4 when compared to the Cyno96h animals. However, both cynomolgus groups had similar percentages of $CD8^+CD107a^+$, $CD8^+IL\text{-}2^+$, or $CD8^+IL\text{-}4^+$ cells, with Cyno96h having higher $CD8^+IFN\text{-}\gamma^+$ levels. To determine whether cellular function was disrupted, we examined cytokine double-positive $CD4^+$ and $CD8^+$ cells. The Cyno96h group had few $CD4^+$ or $CD8^+$ double-positive cells for any combination. The Cyno72h group had higher percentages than the Cyno96h group for all double-positive cytokine combinations in the $CD4^+$ cells but, for the $CD8^+$ double positives, only higher percentages of $CD8^+CD107a^+IFN\text{-}\gamma^+$ and $CD8^+IFN\text{-}\gamma^+IL\text{-}2^+$ cells. The Rhesus72h animals' $CD4^+$ cells expressed high levels of all cytokines compared with the other two groups, including all double-positive combinations. Similarly, high levels of $CD8^+IFN\text{-}\gamma^+$, $CD8^+IL\text{-}2^+$, and $CD8^+IL\text{-}4^+$ were observed compared with the cynomolgus macaques. In contrast, the only high percentages of double-positive cells were for $CD8^+CD107a^+$ and $CD8^+IL\text{-}2^+$ cells expressing IFN-γ. Overall, EBOV-GP–specific T cell responses were detected for all groups.

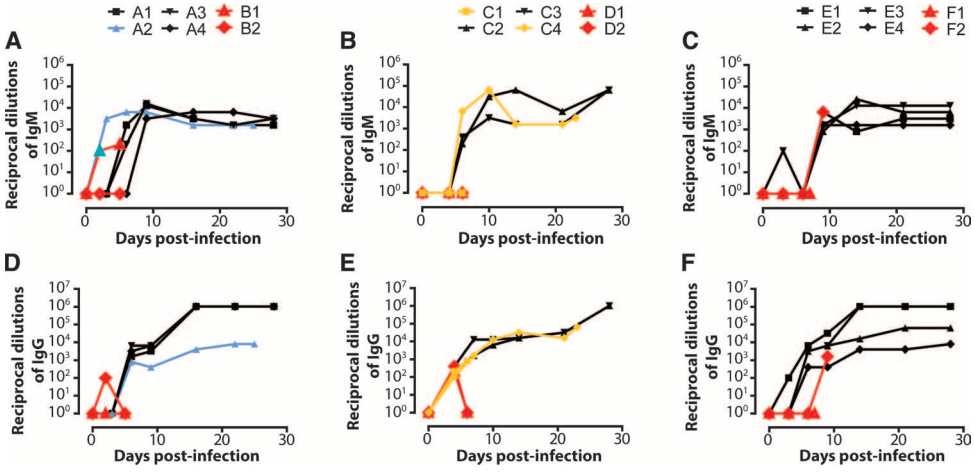

Fig. 4. Ebola-specific antibody responses. (**A** to **F**) Sera from the Cyno72h (A1 to A4), Cyno96h (C1 to C4), and Rhesus72h (E1 to E4) group were quantified by recombinant EBOV-GP ELISA to determine levels of EBOV-GP–specific IgM (A to C) and IgG (D to F), respectively.

DISCUSSION

Early clinical symptoms after EBOV infection are general and resemble that of many other common pathogens where the virus is endemic, such as malaria, cholera, typhoid, and several others (*10*), which make differential diagnosis difficult during an outbreak. By the time positive cases are confirmed by serology (*11*) or qRT-PCR (*12*), prognosis is poor because it is

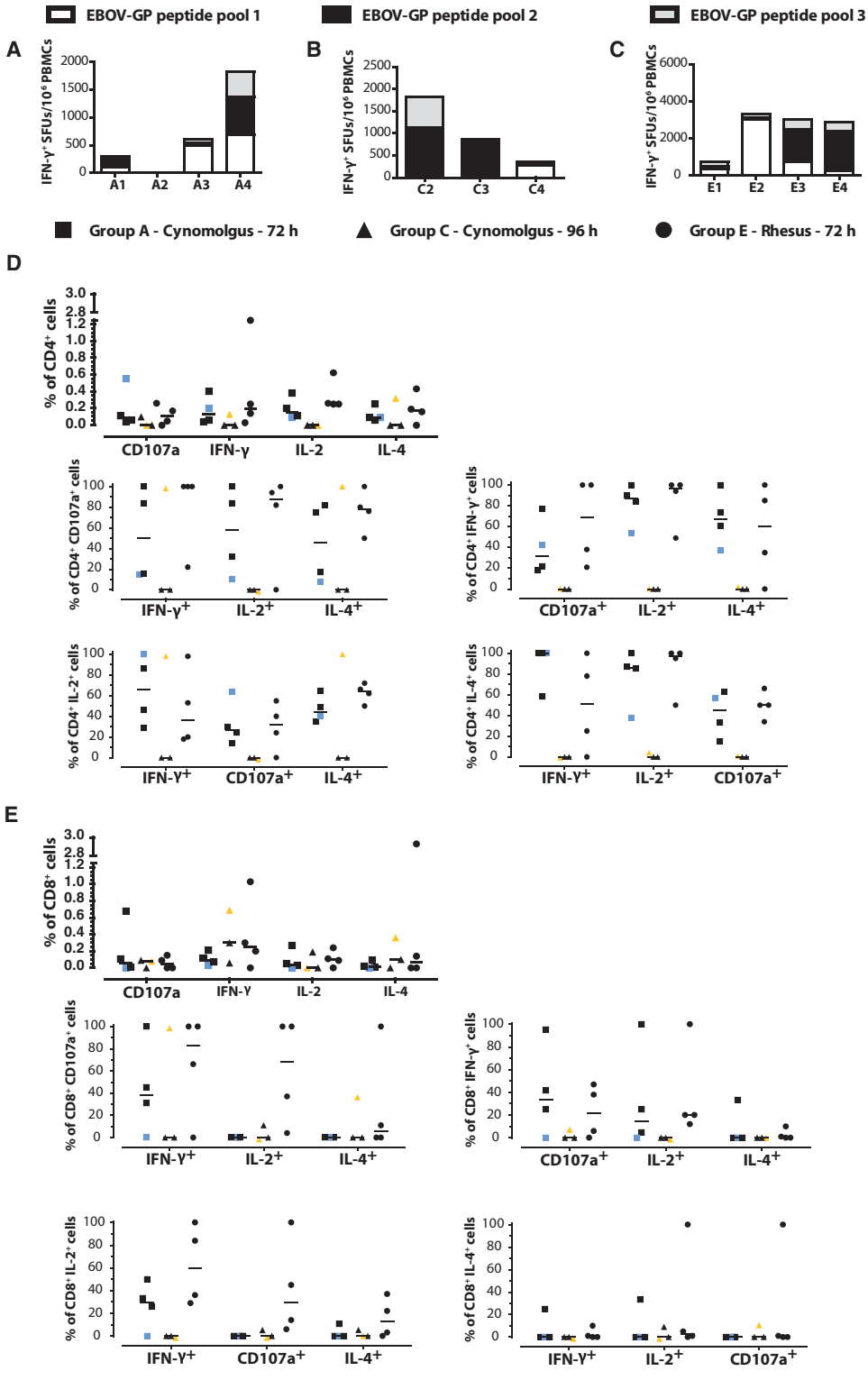

Fig. 5. Ebola-specific T cell responses. PBMCs from each animal still alive at 21 dpi (22 dpi for group A) were stimulated with peptide pools spanning the EBOV surface GP. (**A** to **C**) The production of IFN-γ was assessed by ELISpot for groups A (A), C (B), and E (C). The background number of spots (from a medium-only stimulation) was subtracted from each pool's response. (**D** and **E**) The $CD4^+$ (D) and $CD8^+$ (E) T cell responses were analyzed by flow cytometry. The first larger graphs show the frequencies of cells that are positive for individual cytokines. The four smaller graphs represent the frequencies of cells positive for one marker that are also positive for a second one (for example, the frequency of $CD107a^+$ cells that are also IFN-γ^+). The positivity threshold was defined as two times the background (medium-only stimulation) for the specified gate, in which case the background was subtracted. The responses shown are based on the sum of positive cells for all three pools; the horizontal bar shows the median of each group. Individual animals that died at later time points (A2 and C4) are designated by colored symbols.

already too late to intervene even if the most recent experimental post-exposure treatments were made available. The goal of the current study was to develop and optimize a combination therapy that would be efficacious in NHPs after positive identification of EBOV infection. Rhesus macaques have primarily been used in past post-exposure treatment studies (*2–4*, *13–17*) because they mimic human physiologic and immune responses to EBOV disease (*18*) and succumb a few days later than cynomolgus macaques, thus providing extra time for intervention. Under our conditions, all untreated control cynomolgus and rhesus macaques succumbed to EBOV disease with a mean time to death of 6.04 ± 0.82 dpi (n = 23) versus 7.75 ± 1.26 dpi (n = 4), respectively (fig. S2). Here, both rhesus and cynomolgus macaques were used to test the efficacy of Ad-IFN and ZMAb treatment across both NHP species.

Significant improvement was previously demonstrated with the Ad-IFN and ZMAb combination treatment over ZMAb alone in EBOV-infected guinea pigs (*8*). Ad-IFN toxicity studies in rodents indicate tolerability and meet regulatory requirements. The results presented show that combination therapy with Ad-IFN and ZMAb is 75 and 100% protective in cynomolgus and rhesus macaques, respectively, when administered together at 3 dpi. ZMAb was still 50% effective at 4 dpi, provided Ad-IFN was given at 1 dpi in cynomolgus macaques. Animals could survive lethal infection when treatment was initiated after viremia detection, along with fever presentation. These results show that the Ad-IFN and ZMAb combination treatment is effective after confirmation of EBOV infection by qRT-PCR

and that, at the minimum, it is possible to substantially reduce mortality rates of cases diagnosed early after symptom onset. This treatment significantly extended survival times before euthanasia, over 20 dpi, thereby providing an important opportunity for additional clinical interventions such as those commonly used in intensive care units to control blood chemistry and general homeostasis. In these studies, Ad-IFN was administered through a single intramuscular injection per regimen to conveniently ensure full delivery of the formulation in an animal species that cannot inhale on demand. However, Ad-IFN is intended for delivery in the airway from a nasal spray, a delivery route that was recently shown to overcome existing immunity to homologous adenovirus in rodents and NHPs (*19*, *20*).

Surviving animals across the different groups exhibited robust EBOV-specific B and T cell responses after challenge. The strongest B cell responses were observed in animals receiving Ad-IFN and ZMAb starting at 3 dpi (Cyno72h and Rhesus72h groups) because IgG titers for these animals plateau by 14 dpi, compared to 28 dpi for the Cyno96h NHPs. High EBOV-specific IgG levels were shown to correlate with survival of lethally infected NHPs (*21*). An EBOV-GP–specific T cell response was observed at 21 dpi in both the IFN-γ ELISpot and the intracellular cytokine flow cytometry assays. The Cyno96h group had a higher percentage of $CD8^+$ cells expressing IFN-γ than Cyno72h, which may be attributed to the Cyno96h animals receiving Ad-IFN 48 hours earlier, resulting in the stimulation of a stronger IFN-γ response.

No EBOV escape mutants were detected in any nonsurviving NHPs. Animal C1 aside, the Ad-IFN and ZMAb combination therapy was successful in suppressing viremia in treated NHPs to undetectable levels by 16 dpi. C1 was shown to be especially susceptible to EBOV infection, as evidenced by increased levels of viremia by both $TCID_{50}$ and qRT-PCR detected at 4 dpi compared to other surviving NHPs. It is possible that higher viremia had overwhelmed the treatment regimens, and by 4 dpi, it was already too late for intervention. In contrast, C4 died at 23 dpi despite the presence of comparable B and T cell responses with those of the survivors within its treatment group. However, there was no evidence that this animal succumbed to EBOV disease because viremia was undetectable by both qRT-PCR and $TCID_{50}$, and EBOV could not be isolated by qRT-PCR from oral, rectal, and nasal swabs. PCR of blood targeting the *16S* gene in bacteria was also negative. Symptoms indicative of EBOV disease were not observed at the time of euthanasia, and gross pathology did not reveal any signs of EBOV infection. The cause of death could not be identified, and if it was a result of EBOV infection, it followed an unconventional sequence of events.

A2 had weaker serum IgG levels that did not increase over the course of the experiment after 6 dpi, as well as undetectable levels of IFN-γ–secreting cells coupled with low $CD4^+$ and $CD8^+$ T cell activation. Viremia was cleared by 16 dpi but was then detected again at 22 dpi, coupled with unilateral paralysis. EBOV was detected by qRT-PCR from the cerebrospinal fluid of this animal in similar titers to that detected in the blood, demonstrating that the virus crossed the blood-brain barrier (BBB) into the nervous system. A long-lasting, persistent infection may have been established by EBOV-infected macrophages (*22*), which presumably could cross the BBB, resulting in the evasion of immune responses and accounting for the reemergence of EBOV viremia after its initial drop. This is consistent with a past study, where six treated rhesus macaques that eventually succumbed to EBOV disease at an average of 21.7 dpi exhibited a variety of deteriorating clinical and pathological signs not observed in control animals, in addition to isolation of EBOV antigen in the brain and eye (*23*). Like all other large molecules including recombinant proteins, gene therapeutics, and mAbs (*24*), ZMAb is not expected to cross the BBB readily, and it is questionable that another dose of ZMAb would have changed the survival outcome. However, recent studies have shown that engineered bispecific antibodies targeting β-secretase 1 and transferrin have the ability to cross the BBB (*25*), representing a potential method to overcome this limitation. More in-depth studies, including the susceptibility of neurons and other cells of the central nervous system to EBOV infection, will be necessary to further investigate this phenomenon and its implications on EBOV treatment strategies.

The major limitation of this study is the small number of biological replicates, which affects the power of statistics calculated on all secondary objectives and precludes concluding with accuracy on the significance of close yet different survival rates. This limitation is due to space, reagent, and time when working with containment level 4 (CL4) agents and ethical constraints of working with NHPs. This issue is compounded by the fact that the animals are outbred and not necessarily related to each other, which increases the breadth of observed responses. It is for those reasons that all values are represented in every graph. The next step to refine this successful treatment against Ebola virus infection should include an increase in statistical power. Therefore, future studies will need to focus on a few selected optimal treatments with increased numbers of NHPs per group to compensate for the shortcoming associated with limited biological replicates.

The Ad-IFN and ZMAb combination is shown in the present studies to be effective at treating EBOV disease in both rhesus and cynomolgus macaques. Treatment at the current doses can suppress viremia up to ~10^5 $TCID_{50}$, leading to survival. EBOV viremia could potentially be a measure of prognosis and relative treatment efficacy during an EBOV infection (*26*). Antibody-derived treatments presently offer by far the highest efficacy against EBOV infection in NHPs and boast an excellent safety profile based on the multitude of clinical modalities currently in use to treat several human diseases. Albeit experimental, mAb-based treatments have rapidly been identified by several Biosafety Level 4 programs as the favored clinical option to be included in an emergency response to an accidental EBOV exposure.

MATERIALS AND METHODS

Study design

This study was designed to investigate whether the efficacy of ZMAb treatment after EBOV infection can be improved with a simultaneous Ad-IFN administration, whether the treatment window can be extended after exposure, and whether Ad-IFN + ZMAb treatment is similarly effective in a different NHP species. Our previous study has shown that 50% of cynomolgus macaques can be saved using ZMAb treatment alone when it is administered starting at 48 hours after challenge (*5*). Because of space restrictions and to limited amounts of the ZMAb antibodies, a total of 12 cynomolgus macaques were randomized between four groups: two test groups (n = 4 each) and two control groups (n = 2 each). Six rhesus macaques were randomized in two groups (test group, n = 4; control group, n = 2). The control groups were kept small for humane reasons. After challenge with EBOV, one group of cynomolgus macaques was treated with Ad-IFN + ZMAb starting at 72 hours to test for increased efficacy, one group of cynomolgus

macaques was treated with Ad-IFN 24 hours after challenge before receiving ZMAb starting 96 hours after challenge to test for an extension of the potential treatment window, and the group of rhesus macaques was treated with Ad-IFN + ZMAb starting at 72 hours to test for efficacy in a different NHP species. A number of parameters relevant to survival were monitored over an experimental period of 28 days, including clinical score, viremia by qRT-PCR and $TCID_{50}$ titrations, hematology, blood chemistry, IgG and IgM ELISAs, nAb assays, IFN-γ ELISpot, and flow cytometric ICS assays. This study was not blinded. The study's primary objective is to assess survival rates; all other measurements are considered secondary objectives (clinical disease, immune response, etc.). All assays, except for the flow cytometric ICS, were performed in triplicate. Because there were few animals per group, all values are shown on all graphs.

Viruses and peptides

The challenge virus was Ebola virus H.sapiens-tc/COD/1995/Kikwit-9510621 (EBOV) (order Mononegavirales, family Filoviridae, species *Zaire ebolavirus*; GenBank accession no. AY354458) obtained from the Centers for Disease Control and Prevention (Atlanta, GA), passaged twice on Vero E6 cells cultured in complete minimal essential medium. The reporter virus used for the nAb assay is Ebola virus NML/H.sapiens-lab/COD/1976/Mayinga-eGFP-p3 (EBOV/May-eGFP) (derived from an Ebola virus, family Filoviridae, species *Zaire ebolavirus*; GenBank accession no. NC_002549), which encodes the enhanced green fluorescent protein (eGFP) reporter gene between the NP and VP35 open reading frames. Ad-IFN is a replication-deficient recombinant adenovirus serotype 5 that drives the expression of human IFN-α (*6*), also known as DEF201 (Defyrus Inc.). The peptides (Mimotopes) used as stimulation for T cell assays were 15-mers with an 11–amino acid overlap that spanned the EBOV surface GP. The peptides were combined in three pools as follows: pool 1 has 56 peptides (amino acids 1 to 235), pool 2 has 56 peptides (amino acids 236 to 459), and pool 3 has 55 peptides (amino acids 460 to 676).

Animals

Twelve 2.1- to 5.9-kg cynomolgus macaques (*Macaca fascicularis*) and six 3.1- to 5-kg rhesus macaques (*Macaca mulatta*) were purchased from Primus Bio-Resources. The studies were conducted in the CL4 facility at the Canadian Science Center for Human and Animal Health (CSCHAH), in compliance with the CSCHAH Animal Care Committee following the guidelines of the Canadian Council on Animal Care. The animals were fed standard monkey chow, fruits, vegetables, and treats. Husbandry enrichment consisted of visual stimulation and commercial toys. The subjects were scored daily for signs of disease, and food and water consumption. On treatment days and days 14, 21, and 28, the body temperature and weight were measured, and the following were sampled: blood for serum biochemistry and cell count, Ig detection, and viremia; swabs from the oral, nasal, and rectal cavities. Blood samples for PBMC isolation were collected on day 21 (day 22 for group A) from the surviving animals.

Three individual NHP studies were performed (Table 1). All animals were challenged intramuscularly with 1000 PFU [$1000 \times LD_{50}$ (median lethal dose)] of EBOV (*27*) (1 ml in two sites) on day 0. The Cyno72h (A1 to A4, B1, and B2) and Rhesus72h (E1 to E4, F1, and F2) groups were given Ad-IFN at 1×10^9 PFU/kg at 3 dpi along with ZMAb (50 mg/kg) on 3, 6, and 9 dpi. The Cyno96h (C1 to C4, D1, and D2) group was given Ad-IFN at 1×10^9 PFU/kg at 1 dpi and ZMAb (50 mg/kg) at 4, 7, and 10 dpi. The two controls in each of cynomolgus studies were given different mock treatments on the same treatment dates as their respective group. Controls B2 and D2 received PBS. Control B1 received mouse IgG (50 mg/kg) (Lampire Biological) in PBS–100 mM sucrose at 2 dpi, whereas control D1 received PBS at 1 dpi, and the mouse IgG at 4 dpi. One of the two rhesus controls (F1) received mouse IgG (Equitech-Bio Inc.), whereas the other (F2) received Ad-IFN at 1×10^9 PFU/kg at 3 dpi.

EBOV-GP–specific neutralizing mAb production

The development and characterization of the EBOV-GP–specific neutralizing mAbs in the ZMAb treatment were described previously (*28*, *29*). The large-scale production was conducted by the Biotechnology Research Institute. Mouse hybridomas were grown in Hybridoma SFM (Invitrogen) and 1% ultralow IgG fetal bovine serum (FBS) (Invitrogen) in 45-liter batches for 5 days. After centrifugation, the supernatant was clarified with cartridge filters and then concentrated 10 times by tangential flow filtration (TFF) with a 30-kD Omega Centrasette II cassette (Pall Corp.). The concentrate was diafiltered against 5 volumes of protein G binding buffer (20 mM NaH_2PO_4, 0.15 M NaCl at pH 8.0). This feedstock was loaded on an equilibrated protein G–Sepharose 4FF column and washed with binding buffer until the ultraviolet absorbance returned to baseline, and the mAb was eluted with 0.1 M glycine and 0.15 M NaCl (pH 2.8), which was immediately neutralized with 1 M tris (pH 8.8). The purified IgG fractions were pooled and concentrated by TFF to 20 to 30 mg/ml and then diafiltered against 5 volumes of PBS. The final product was sterile-filtered on a 0.22-μm filter and stored at −80°C. Protein concentration and purity were assessed by high-performance liquid chromatography, purity was 97 to 99%, and endotoxin levels were <2 to 8.8 endotoxin units/ml. The antibodies were combined and diluted before injection to a final concentration of 20 mg/ml; to improve solubility, we added concentrated sucrose in Dulbecco's PBS (HyClone) to a final concentration of 100 mM sucrose.

Enzyme-linked immunosorbent assay

ELISAs for monkey IgG and IgM were performed as described previously (*30*), with a recombinant EBOV-GPΔTM (IBT Bioservices) as a capture antigen. The assays were performed once with each sample assayed in triplicate. A dilution was considered positive if its mean value was at least 2 SDs above the mean of a similar day 0 dilution.

EBOV titration

The $TCID_{50}$ for each time point was determined by adding 10-fold serial dilutions of whole blood to Vero E6 cells with four replicates per dilution. The plates were scored for cytopathic effect at 14 dpi, and the titers were calculated with the Reed and Muench method (*31*).

For titers as measured by genome copies, total RNA was extracted from whole blood with the QIAmp Viral RNA Mini Kit (Qiagen). EBOV was detected by qRT-PCR with the LightCycler 480 RNA Master Hydrolysis Probes (Roche) assay targeting the RNA polymerase (nucleotides 16472 to 16538, AF086833). The reaction conditions were as follows: 63°C for 3 min, 95°C for 30 s, and cycling of 95°C for 15 s, 60°C for 30 s for 45 cycles with a LightCycler 480 II (Roche). The lower detection limit for this assay is 86 GECs/ml. The primer sequences were as follows: EBOVLF2 (CAGCCAGCAATTTCTTCCAT), EBOVLR2 (TTTCGGTTGCTGTTTCTGTG), and EBOVLP2FAM (FAM-ATCATTGGCGTACTGGAGGAGCAG-BHQ1).

EBOV/May-eGFP–neutralizing antibody assays

Sera were inactivated for 45 min at 56°C and serially diluted twofold with Dulbecco's modified Eagle's medium in triplicate. Diluted sera were incubated at 37°C for 60 min with an equal volume of EBOV/May-eGFP (100 PFU per well). The mixture was added to Vero E6 cells and incubated at 37°C for 48 hours. The plates were fixed with 10% phosphate-buffered formalin. eGFP fluorescence was quantified with a fluorescence plate reader (Advanced Imaging Devices). The highest serum dilution to reduce the fluorescence signal by at least 50% was considered to be the endpoint titer. Neutralization titers are reported as reciprocal of this dilution.

Cytokine assays

For cynomolgus macaques, PBMCs were isolated by centrifuging whole blood at 1200*g* for 10 min and then diluting the buffy coat in RPMI before layering onto 60% Percoll (GE Healthcare) and centrifuged at 500*g* for 30 min. The band at the medium-Percoll interface was harvested and washed once with RPMI and resuspended in cRPMI (RPMI 1640, 1 mM L-glutamine, 50 μM β-mercaptoethanol, 10% FBS, and 1% penicillin/streptomycin).

For rhesus macaques, PBMCs were isolated by diluting whole blood with PBS (1:2) and layering the diluted blood on Ficoll (GE Healthcare) and centrifuging at 400*g* for 40 min. The band at the PBS-Ficoll interface was harvested and washed once in PBS and twice in L15 medium (HyClone). The cells were resuspended in cRPMI.

IFN-γ ELISpot assays (BD Biosciences) were performed in triplicate according to the manufacturer's protocol with 5×10^5 PBMCs per well in cRPMI. Three peptide pools were used for stimulation (2.5 μg/ml) and incubated for 18 hours. Spots were visualized with the AEC substrate (BD Biosciences) and quantified with the ELISpot Plate Reader (AID Cell Technology).

The frequency of $CD4^+$ or $CD8^+$ cells producing IFN-γ, IL-2, IL-4, and CD107a was assessed by flow cytometry using the following antibodies: CD3 Alexa Fluor 700 (clone SP34-2) and CD4 peridinin chlorophyll protein (PerCP)–Cy5.5 (clone L200) from BD Biosciences; CD8 phycoerythrin (PE)–Cy7 (clone RPA-T8), CD107a Brilliant Violet 421 (clone H4A3), IL-2 Alexa Fluor 488 (clone MQ1-17h12), IL-4 PE (clone 8D4-8), and IFN-γ allophycocyanin (APC) (clone B27) from BioLegend. One million PBMCs were stimulated overnight with peptides (5 μg/ml), using GolgiPlug (0.5 μl/ml) and GolgiStop (0.6 μl/ml), in the presence of the anti-CD107a antibody. After surface staining (for CD3, CD4, and CD8), the samples were incubated twice for 30 min in Cytofix/Cytoperm (BD Biosciences) for permeabilization and removal from CL4. ICS was performed, and the samples were kept overnight in PBS–1% formaldehyde. Then, 250,000 to 500,000 events were acquired on a BD LSR II, and the data were analyzed with FlowJo vX.0.6.

PCR of blood for the *16S* gene

Whole blood was lysed in AVL buffer (Qiagen) and removed from CL4 as per the appropriate standard operating procedures. The DNA was extracted, and the purified genomic DNA was used in a PCR with the primers pA and pDr (*32*). The reaction was run on an agarose gel and, if a product was present, sent for sequencing. The PCR conditions were as follows: the reaction used the Platinum Taq enzyme (Invitrogen); 5% dimethyl sulfoxide; cycling conditions: 94°C for 5 min, 35 cycles of 94°C for 1 min, 55°C for 1 min, 72°C for 1 min, final extension of 72°C for 10 min.

Statistics

Survival was assessed with the log-rank test; for rhesus macaques, four historical controls were included in the control group, whereas the two cynomolgus macaque control groups (groups B and D) were grouped together for the statistical analysis; the statistics were calculated with GraphPad Prism 5. For IgG and IgM ELISAs, a positive signal was defined as an optical density value at least 2 SDs above a similar dilution of the day 0 serum for the same animal. For the ELISpot assay, positive signal was determined by subtracting the average medium-only count from the average peptide-stimulated count. For fluorescence-activated cell sorting, medium-only frequencies were subtracted from the peptide-stimulated frequencies if the stimulated samples had frequencies at least twice that of the medium-only sample. The sum of the three peptide pools is presented.

SUPPLEMENTARY MATERIALS

www.sciencetranslationalmedicine.org/cgi/content/full/5/207/207ra143/DC1
Fig. S1. EBOV/May-eGFP–neutralizing antibody assays.
Fig. S2. Survival curves and time to death of historical control rhesus and cynomolgus macaques.
Table S1. Ebola viremia values at various times post-challenge as measured by qRT-PCR.
Table S2. Viremia by $TCID_{50}$.
Table S3. Clinical score.
Table S4. Temperature.
Table S5. ALT.
Table S6. ALP.
Table S7. PLT.
Table S8. WBCs.
Table S9. PCR results for animal C4 for EBOV and 16*S* DNA.
Table S10. IgM titers.
Table S11. IgG titers.
Table S12. nAb titers.
Table S13. ELISpot counts.
Table S14. Cytokine positivity of $CD8^+$ cells.
Table S15. Cytokine positivity of $CD8^+$ $CD107a^+$ cells.
Table S16. Cytokine positivity of $CD8^+$ $IL\text{-}2^+$ cells.
Table S17. Cytokine positivity of $CD8^+$ $IFN\text{-}\gamma^+$ cells.
Table S18. Cytokine positivity of $CD8^+$ $IL\text{-}4^+$ cells.
Table S19. Cytokine positivity of $CD4^+$ cells.
Table S20. Cytokine positivity of $CD4^+$ $CD107a^+$ cells.
Table S21. Cytokine positivity of $CD4^+$ $IL\text{-}2^+$ cells.
Table S22. Cytokine positivity of $CD4^+$ $IFN\text{-}\gamma^+$ cells.
Table S23. Cytokine positivity of $CD4^+$ $IL\text{-}4^+$ cells.

REFERENCES AND NOTES

1. J. A. Wilson, C. M. Bosio, M. K. Hart, Ebola virus: The search for vaccines and treatments. *Cell. Mol. Life Sci.* **58**, 1826–1841 (2001).
2. J. M. Dye, A. S. Herbert, A. I. Kuehne, J. F. Barth, M. A. Muhammad, S. E. Zak, R. A. Ortiz, L. I. Prugar, W. D. Pratt, Postexposure antibody prophylaxis protects nonhuman primates from filovirus disease. *Proc. Natl. Acad. Sci. U.S.A.* **109**, 5034–5039 (2012).
3. A. Marzi, R. Yoshida, H. Miyamoto, M. Ishijima, Y. Suzuki, M. Higuchi, Y. Matsuyama, M. Igarashi, E. Nakayama, M. Kuroda, M. Saijo, F. Feldmann, D. Brining, H. Feldmann, A. Takada, Protective efficacy of neutralizing monoclonal antibodies in a nonhuman primate model of Ebola hemorrhagic fever. *PLoS One* **7**, e36192 (2012).
4. G. G. Olinger Jr., J. Pettitt, D. Kim, C. Working, O. Bohorov, B. Bratcher, E. Hiatt, S. D. Hume, A. K. Johnson, J. Morton, M. Pauly, K. J. Whaley, C. M. Lear, J. E. Biggins, C. Scully, L. Hensley, L. Zeitlin, Delayed treatment of Ebola virus infection with plant-derived monoclonal antibodies provides protection in rhesus macaques. *Proc. Natl. Acad. Sci. U.S.A.* **109**, 18030–18035 (2012).
5. X. Qiu, J. Audet, G. Wong, S. Pillet, A. Bello, T. Cabral, J. E. Strong, F. Plummer, C. R. Corbett, J. B. Alimonti, G. P. Kobinger, Successful treatment of Ebola virus–infected cynomolgus macaques with monoclonal antibodies. *Sci. Transl. Med.* **4**, 138ra81 (2012).
6. J. Q. Wu, N. D. Barabé, Y. M. Huang, G. A. Rayner, M. E. Christopher, F. L. Schmaltz, Pre- and post-exposure protection against *Western equine encephalitis virus* after single inoculation with adenovirus vector expressing interferon alpha. *Virology* **369**, 206–213 (2007).

7. J. S. Richardson, G. Wong, S. Pillet, S. Schindle, J. Ennis, J. Turner, J. E. Strong, G. P. Kobinger, Evaluation of different strategies for post-exposure treatment of Ebola virus infection in rodents. *J. Bioterror. Biodef.* (S1), 007 (2011).
8. X. Qiu, G. Wong, L. Fernando, J. Ennis, J. D. Turner, J. B. Alimonti, X. Yao, G. P. Kobinger, Monoclonal antibodies combined with adenovirus-vectored interferon significantly extend the treatment window in Ebola virus-infected guinea pigs. *J. Virol.* **87**, 7754–7757 (2013).
9. E. I. Ryabchikova, L. V. Kolesnikova, S. V. Luchko, An analysis of features of pathogenesis in two animal models of Ebola virus infection. *J. Infect. Dis.* **179** (Suppl. 1), S199–S202 (1999).
10. J. H. Gear, Clinical aspects of African viral hemorrhagic fevers. *Rev. Infect. Dis.* **11** (Suppl. 4), S777–S782 (1989).
11. T. G. Ksiazek, P. E. Rollin, P. B. Jahrling, E. Johnson, D. W. Dalgard, C. J. Peters, Enzyme immunosorbent assay for Ebola virus antigens in tissues of infected primates. *J. Clin. Microbiol.* **30**, 947–950 (1992).
12. E. M. Leroy, S. Baize, C. Y. Lu, J. B. McCormick, A. J. Georges, M. C. Georges-Courbot, J. Lansoud-Soukate, S. P. Fisher-Hoch, Diagnosis of Ebola haemorrhagic fever by RT-PCR in an epidemic setting. *J. Med. Virol.* **60**, 463–467 (2000).
13. L. M. Smith, L. E. Hensley, T. W. Geisbert, J. Johnson, A. Stossel, A. Honko, J. Y. Yen, J. Geisbert, J. Paragas, E. Fritz, G. Olinger, H. A. Young, K. H. Rubins, C. L. Karp, Interferon-β therapy prolongs survival in rhesus macaque models of Ebola and Marburg hemorrhagic fever. *J. Infect. Dis.* **208**, 310–318 (2013).
14. H. Feldmann, S. M. Jones, K. M. Daddario-DiCaprio, J. B. Geisbert, U. Ströher, A. Grolla, M. Bray, E. A. Fritz, L. Fernando, F. Feldmann, L. E. Hensley, T. W. Geisbert, Effective post-exposure treatment of Ebola infection. *PLoS Pathog.* **3**, e2 (2007).
15. T. W. Geisbert, A. C. Lee, M. Robbins, J. B. Geisbert, A. N. Honko, V. Sood, J. C. Johnson, S. de Jong, I. Tavakoli, A. Judge, L. E. Hensley, I. Maclachlan, Postexposure protection of non-human primates against a lethal Ebola virus challenge with RNA interference: A proof-of-concept study. *Lancet* **375**, 1896–1905 (2010).
16. T. K. Warren, K. L. Warfield, J. Wells, D. L. Swenson, K. S. Donner, S. A. Van Tongeren, N. L. Garza, L. Dong, D. V. Mourich, S. Crumley, D. K. Nichols, P. L. Iversen, S. Bavari, Advanced antisense therapies for postexposure protection against lethal filovirus infections. *Nat. Med.* **16**, 991–994 (2010).
17. T. W. Geisbert, L. E. Hensley, P. B. Jahrling, T. Larsen, J. B. Geisbert, J. Paragas, H. A. Young, T. M. Fredeking, W. E. Rote, G. P. Vlasuk, Treatment of Ebola virus infection with a recombinant inhibitor of factor VIIa/tissue factor: A study in rhesus monkeys. *Lancet* **362**, 1953–1958 (2003).
18. N. A. Twenhafel, M. E. Mattix, J. C. Johnson, C. G. Robinson, W. D. Pratt, K. A. Cashman, V. Wahl-Jensen, C. Terry, G. G. Olinger, L. E. Hensley, A. N. Honko, Pathology of experimental aerosol *Zaire ebolavirus* infection in rhesus macaques. *Vet. Pathol.* **50**, 514–529 (2013).
19. M. A. Croyle, A. Patel, K. N. Tran, M. Gray, Y. Zhang, J. E. Strong, H. Feldmann, G. P. Kobinger, Nasal delivery of an adenovirus-based vaccine bypasses pre-existing immunity to the vaccine carrier and improves the immune response in mice. *PLoS One* **3**, e3548 (2008).
20. J. S. Richardson, S. Pillet, A. J. Bello, G. P. Kobinger, Airway delivery of an adenovirus-based Ebola virus vaccine bypasses existing immunity to homologous adenovirus in nonhuman primates. *J. Virol.* **87**, 3668–3677 (2013).
21. G. Wong, J. S. Richardson, S. Pillet, A. Patel, X. Qiu, J. Alimonti, J. Hogan, Y. Zhang, A. Takada, H. Feldmann, G. P. Kobinger, Immune parameters correlate with protection against ebola virus infection in rodents and nonhuman primates. *Sci. Transl. Med.* **4**, 158ra146 (2012).
22. M. Bray, T. W. Geisbert, Ebola virus: The role of macrophages and dendritic cells in the pathogenesis of Ebola hemorrhagic fever. *Int. J. Biochem. Cell Biol.* **37**, 1560–1566 (2005).
23. T. Larsen, E. L. Stevens, K. J. Davis, J. B. Geisbert, K. M. Daddario-DiCaprio, P. B. Jahrling, L. E. Hensley, T. W. Geisbert, Pathologic findings associated with delayed death in nonhuman primates experimentally infected with Zaire Ebola virus. *J. Infect. Dis.* **196** (Suppl. 2), S323–S328 (2007).
24. W. M. Pardridge, The blood-brain barrier: Bottleneck in brain drug development. *NeuroRx* **2**, 3–14 (2005).
25. J. K. Atwal, Y. Chen, C. Chiu, D. L. Mortensen, W. J. Meilandt, Y. Liu, C. E. Heise, K. Hoyte, W. Luk, Y. Lu, K. Peng, P. Wu, L. Rouge, Y. Zhang, R. A. Lazarus, K. Scearce-Levie, W. Wang, Y. Wu, M. Tessier-Lavigne, R. J. Watts, A therapeutic antibody targeting BACE1 inhibits amyloid-β production in vivo. *Sci. Transl. Med.* **3**, 84ra43 (2011).
26. A. Sanchez, M. Lukwiya, D. Bausch, S. Mahanty, A. J. Sanchez, K. D. Wagoner, P. E. Rollin, Analysis of human peripheral blood samples from fatal and nonfatal cases of Ebola (Sudan) hemorrhagic fever: Cellular responses, virus load, and nitric oxide levels. *J. Virol.* **78**, 10370–10377 (2004).
27. P. B. Jahrling, T. W. Geisbert, J. B. Geisbert, J. R. Swearengen, M. Bray, N. K. Jaax, J. W. Huggins, J. W. LeDuc, C. J. Peters, Evaluation of immune globulin and recombinant interferon-α2b for treatment of experimental Ebola virus infections. *J. Infect. Dis.* **179** (Suppl. 1), S224–S234 (1999).
28. X. Qiu, J. B. Alimonti, P. L. Melito, L. Fernando, U. Ströher, S. M. Jones, Characterization of *Zaire ebolavirus* glycoprotein-specific monoclonal antibodies. *Clin. Immunol.* **141**, 218–227 (2011).
29. X. Qiu, L. Fernando, P. L. Melito, J. Audet, H. Feldmann, G. Kobinger, J. B. Alimonti, S. M. Jones, Ebola GP-specific monoclonal antibodies protect mice and guinea pigs from lethal Ebola virus infection. *PLoS Negl. Trop. Dis.* **6**, e1575 (2012).
30. X. Qiu, L. Fernando, J. B. Alimonti, P. L. Melito, F. Feldmann, D. Dick, U. Ströher, H. Feldmann, S. M. Jones, Mucosal immunization of cynomolgus macaques with the VSVΔG/ZEBOVGP vaccine stimulates strong Ebola GP-specific immune responses. *PLoS One* **4**, e5547 (2009).
31. L. J. Reed, H. Muench, A simple method of estimating fifty per cent endpoints. *Am. J. Hyg.* **27**, 493–497 (1938).
32. U. Edwards, T. Rogall, H. Blöcker, M. Emde, E. C. Böttger, Isolation and direct complete nucleotide determination of entire genes. Characterization of a gene coding for 16S ribosomal RNA. *Nucleic Acids Res.* **17**, 7843–7853 (1989).

Acknowledgments: We thank J. Gren, S. Jones, A. Grolla, D. Kobasa, T. Cutts, and J. Richardson for their excellent technical assistance, as well as J. Turner and J. Ennis for providing the Ad-IFN used in these studies. **Funding:** This research was supported by the Public Health Agency of Canada and funded by a grant from the Chemical, biological, radiological and nuclear, CBRN, Research and Technology Initiative to G.P.K. G.W. is the recipient of a Doctoral Research Award from the Canadian Institute for Health Research. **Author contributions:** X.Q. designed and conducted the experiments and wrote the paper. G.W., J.A., and J.B.A. conducted the experiments and wrote the paper. L.F., A.B., and J.S. conducted the experiments. G.P.K. designed and conducted the experiments and wrote the paper. **Competing interests:** Her Majesty the Queen in right of Canada holds a patent on the mAbs 1H3, 2G4, and 4G7, PCT/CA2009/000070, "Monoclonal antibodies for Ebola and Marburg viruses." The authors declare no other competing interests. **Data and materials availability:** The mAbs are available pending a materials transfer agreement.

Submitted 17 May 2013
Accepted 22 August 2013
Published 16 October 2013
10.1126/scitranslmed.3006605

Citation: X. Qiu, G. Wong, L. Fernando, J. Audet, A. Bello, J. Strong, J. B. Alimonti, G. P. Kobinger, mAbs and ad-vectored IFN-α therapy rescue Ebola-infected nonhuman primates when administered after the detection of viremia and symptoms. *Sci. Transl. Med.* **5**, 207ra143 (2013).

Science Translational Medicine

mAbs and Ad-Vectored IFN-α Therapy Rescue Ebola-Infected Nonhuman Primates When Administered After the Detection of Viremia and Symptoms

Xiangguo Qiu, Gary Wong, Lisa Fernando, Jonathan Audet, Alexander Bello, Jim Strong, Judie B. Alimonti and Gary P. Kobinger

Sci Transl Med **5**, 207ra143207ra143.
DOI: 10.1126/scitranslmed.3006605

Every Day Counts

Ebola virus (EBOV) infections cause a deadly hemorrhagic disease for which there are no currently licensed vaccines or treatments. Recent studies have demonstrated the potential of antibody therapy cocktails (ZMAb) for treating EBOV infections; however, there is a limited time window for these therapies to be effective. Because early clinical symptoms of EBOV infection resemble other common pathogens, it is critical to extend this treatment window until positive cases can be confirmed. Now, Qui *et al.* combine ZMAb therapy with adenovirally delivered interferon- α (Ad-IFN) to extend the EBOV treatment window in nonhuman primates.

The authors dosed macaques that had received a lethal dose of EBOV with a combination of ZMAb and Ad-IFN. Combination therapy with Ad-IFN and ZMAb was 75 and 100% protective in cynomolgus and rhesus macaques, respectively, when administered together at 3 days post-infection. Fifty percent of cynomolgus macaques were protected at 4 days post-infection when Ad-IFN was administered 1 day post-infection. These results suggest that the Ad-IFN and ZMAb combination treatment could be effective after confirmation of EBOV infection as well as could substantially reduce mortality rates of cases diagnosed early after symptom onset.